Massive Boson Production at Small q$_T$ in Soft-Collinear Effective Theory

Thomas Becher[a], Matthias Neubert[b], Daniel Wilhelm[b]

[a]*Institut für Theoretische Physik, Universität Bern, Switzerland*
[b]*Institut für Physik (THEP), Johannes Gutenberg-Universität Mainz, Germany*

Abstract

We study the differential cross sections for electroweak gauge-boson and Higgs production at small and very small transverse-momentum q_T. Large logarithms are resummed using soft-collinear effective theory. The collinear anomaly generates a non-perturbative scale q_*, which protects the processes from receiving large long-distance hadronic contributions. A numerical comparison of our predictions with data on the transverse-momentum distribution in Z-boson production at the Tevatron and LHC is given.

1. Drell-Yan-Like Processes

Historically the Drell-Yan (DY) process [1] denoted the inclusive production of a virtual photon by quark-antiquark annihilation in hadron collisions and the subsequent decay into a lepton pair. Its main features are strongly coupled initial and color-neutral final states and so the photon case can easily be generalized to W- and Z-boson production. Even the Higgs production via gluon fusion can be described in a similar way.

The transverse-momentum distribution of DY-like processes is one of the most basic observables at hadron colliders. It is used e.g. to extract the W-boson mass and width and is of great phenomenological relevance for Higgs-production at the LHC. Especially the regime of small transverse-momentum $q_T^2 \ll M^2$ is important, because it gives the largest contribution to the total cross section. Here q_T denotes the transverse component of the boson 4-momentum q, while M^2 is its invariant mass q^2. We thus consider:

$$\frac{d\sigma}{dq_T} \quad \text{with} \quad q^2 = M^2 \gg q_T^2 \gg \Lambda_{QCD}^2 .$$

The hierarchy in this regime between the hard scale M and the collinear scale q_T leads to large logarithms which spoil the perturbativity of fixed-order calculations. These logarithms need to be resummed to all orders in perturbation theory to achieve a predictive result. Our approach [2] is to factorize the cross section using an effective field theory (EFT) and resum large logarithms via renormalization group (RG) techniques. The appropriate EFT to describe DY-like processes is the soft-collinear effective theory (SCET) [3], because it ac-

counts for the complex structure of underlying scales originating from Sudakov double logarithms [4].

2. Factorization using SCET

SCET is an EFT of QCD. In general it describes any number of collinear modes, high energetic particles (or Jets) with light-like momenta and soft modes, which mediate the only interactions between the different collinear fields.
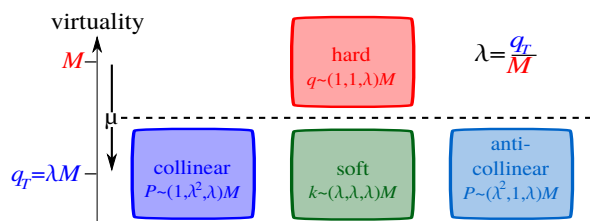

Figure 1: Momentum modes in SCET.

In DY-like processes there are two collinear modes, defined by the two opposite light-like momenta of the colliding hadrons. The different momentum regions are best defined in lightcone coordinates. Therefore we introduce two light-like reference vectors n and $\bar{n}$ along the beam axis with $n \cdot \bar{n} = 2$. Now every 4-vector k can be decomposed into its collinear (k_+), anti-collinear (k_-) and perpendicular ($k_\perp$) component, by projecting it onto n and $\bar{n}$.

The values of interest are the virtuality $\sqrt{k^2}$ and the scalings of momenta:

$$\text{Scaling:} \quad k \sim (k_+, k_-, k_T) \quad \text{with} \quad k_T^2 = -k_\perp^2 .$$
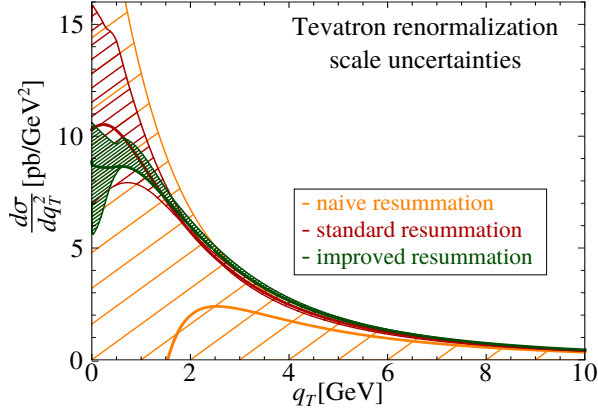
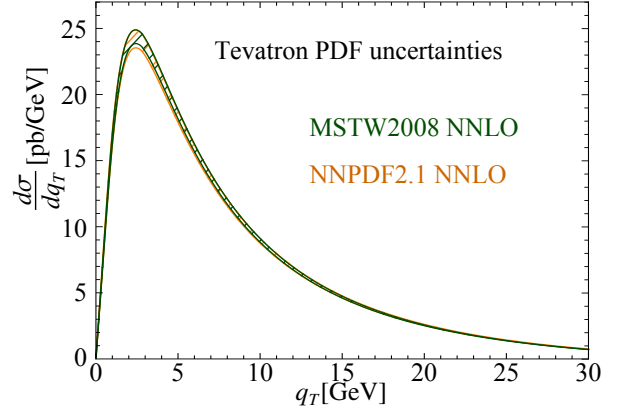Figure 2: Scale uncertainties for different resummation schemes.

Figure 3: PDF uncertainties for different PDF sets.

A virtuality of $\mathcal{O}(M)$ identifies the hard modes, which are integrated out like the produced DY-boson. The scaling is used to distinguish between the different collinear and soft modes (Figure 1).

Up to power suppressed terms, the factorization using SCET leads to the following double differential cross section, where y denotes the rapidity of the DY-boson:

$$\frac{\mathrm{d}^2\sigma}{\mathrm{d}q_T \mathrm{d}y} \sim H \cdot \sum_{ij} Q_{ij} \cdot \int \mathrm{d}^2\vec{x}_\perp \; \mathrm{e}^{-i\vec{q}_\perp \cdot \vec{x}_\perp} \cdot W \cdot \mathcal{B}_{i/N_1}\mathcal{B}_{j/N_2} \, .$$

It consists of a hard function H, a sum over contributing partons and effective charges, a soft function W and two collinear functions $\mathcal{B}$. The hard function contains the Wilson coefficients of the EFT. The soft function leads to scaleless integrals, thus does not contribute to all orders in perturbation theory:

$$H(M,\mu) = \left|C(-M^2,\mu^2)\right|^2, \qquad W = 1 + \mathcal{O}(\lambda^2) \, .$$

Comparing the collinear functions $\mathcal{B}$ with the representation of ordinary parton distribution functions (PDF) in SCET, it turns out they are just generalized x_T dependent PDFs (gPDF):

$$\mathcal{B}_{q/N}(\xi,L_\perp) = \int \frac{\mathrm{d}t}{2\pi} \; \mathrm{e}^{-itnp} \langle N| \bar{\chi}_c(nt + x_\perp)\frac{\not{n}}{2}\chi_c(0) |N\rangle \, .$$

Here the x_T and μ dependence is hidden in the logarithm $L_\perp = \ln\left(x_T^2\mu^2\right)$. The Wilson coefficients are known, the soft corrections vanish and one can match the gPDFs on partonic level onto ordinary PDFs, only missing long-distance hadronic effects of $\mathcal{O}\left(\Lambda_{NP}^2 x_T^2\right)$:

$$\mathcal{B}_{i/N}(\xi,L_\perp) = \sum_j \int_\xi^1 \frac{\mathrm{d}z}{z} \, \mathcal{I}_{ij}(z,L_\perp)\phi_{j/N}(\tfrac{\xi}{z},\mu) \, .$$

3. Collinear Anomaly and Resummation

On the classical level the SCET Lagrangian respects the so-called rescaling symmetry. Since the two collinear fields can not interact with each other, each of their Lagrangians is invariant under the rescaling of momenta of the other one. At higher orders the collinear anomaly (CA) appears, the symmetry is broken by quantum corrections and restricted to joint rescaling, which introduces an unexpected invariant:

$$\begin{aligned} \mathcal{L}_c : \quad & \bar{p} \rightarrow \bar{\alpha}\bar{p} \\ \mathcal{L}_{\bar{c}} : \quad & p \rightarrow \alpha p \end{aligned} \xrightarrow{CA} \alpha \cdot \bar{\alpha} \equiv 1 \quad \Rightarrow \quad M^2 = 2p\bar{p} \, .$$

It turns out that this directly effects the matching of the gPDFs by generating a power-like dependence on the hard scale M:

$$\mathcal{B}_{i/N}\mathcal{B}_{j/N} \xrightarrow{CA} (x_T^2 M^2)^{F_{ij}(L_\perp)} B_{i/N}(\xi,L_\perp)B_{j/N}(\xi,L_\perp) \, .$$

This term ensures the RG invariance in the absence of soft contributions and is important for the resummation of large logarithms.

The resummation of the hard function is simply done by using the RG equation:

$$H(M,\mu) = H(M,\mu_h) \cdot U(\mu_h,\mu) \quad \text{and set} \quad \mu_h \sim M \, .$$

Resumming the terms under the Fourier integral,

$$\int \mathrm{d}x_T^2 \; \mathrm{e}^{-iq_T x_T} (x_T^2 M^2)^{F_{ij}(L_\perp)} B_{i/N}(\xi,L_\perp)B_{j/N}(\xi,L_\perp) \, ,$$

is more subtle. It contains two types of logarithms, $L_\perp = \ln\left(x_T^2\mu^2\right)$ from the collinear modes and $\ln\frac{M^2}{\mu^2}$ from the CA. Setting $\mu \sim q_T$ and expanding in α_s leads to small $L_\perp$, because x_T is the conjugate variable of q_T under the Fourier integral. At small q_T this naive resummation scheme leads to a large logarithm contained
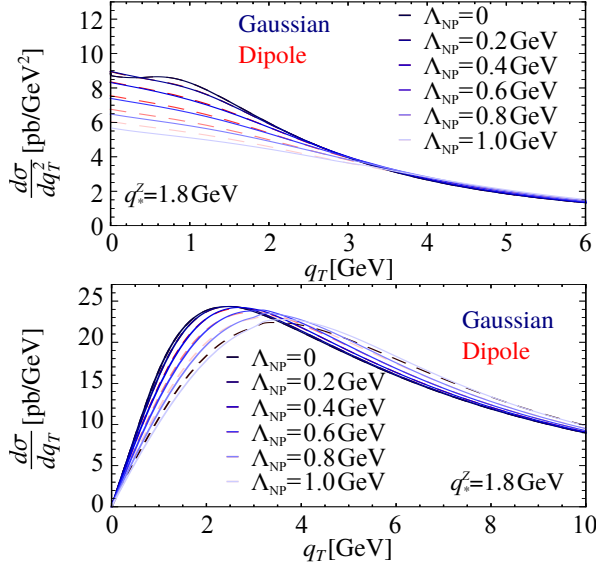
2

Figure 4: Impact of hadronic effects on the intercept (top) and the peak-region (bottom) for Z-production.

Figure 5: Impact of hadronic effects on the intercept (top) and the peak-region (bottom) for Higgs-production.

in $\eta \sim \alpha_s \ln \frac{M^2}{\mu^2}$, which spoils the perturbativity.

To avoid this, our standard resummation scheme is to count η as $O(1)$ and include higher order terms (in α_s) of the CA.

The standard resummation breaks down when η reaches 1. This happens at the scale q_*:

$$q_*^Z \approx 1.8\,\text{GeV}, \qquad q_*^H \approx 7.7\,\text{GeV}.$$

To lower q_T beyond q_* one has to dismiss the demand of small $L_\perp$ by setting $\mu \sim q_*$. The appearing higher order terms of the CA form a Gaussian under the integral, which regulates it independently of q_T, even at vanishing transverse-momentum $q_* \gg \Lambda_{QCD} > q_T \geqslant 0$.

4. Uncertainties

The first plot (Figure2) shows the renormalization scale uncertainties for Z-boson production at the Tevatron. The error bands correspond to varying the default renormalization scale $\mu_d = q_T + q_*^Z$ by a factor of two. The errors of the naive resummation (orange) lead to unpredictive results, because the terms of the CA are missing. The standard resummation (red) gives considerable smaller error bands. The errors of the improved resummation (green) are somewhat smaller above q_*^Z, but significantly below. As a consequence all following plots are made using the improved resummation scheme.

The second plot (Figure 3) shows the PDF uncertainties for two different PDF sets at the Tevatron. The different shape of the plot depends on showing $\frac{d\sigma}{dq_T}$ instead
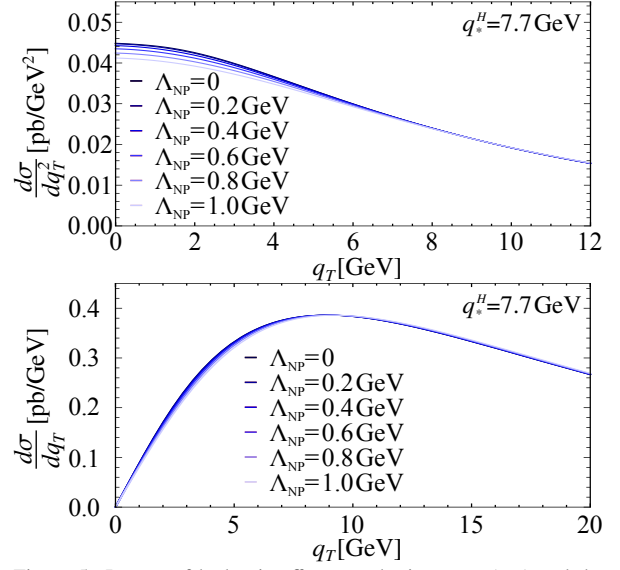
of $\frac{d\sigma}{dq_T^2}$. The first is used to point out the peak region, the latter for the intercept. The error bands correspond to one standard deviation to the center value. The uncertainties are around 5%, therefore lie within the renormalization scale uncertainties.

The hard function is independent of q_T, thus can be regarded as an overall factor with constant uncertainties (Table 1). In the following plots the error bands correspond to the scale uncertainty.

	$\mu_h^2 = m_Z^2$	$\mu_h^2 = -m_Z^2$
NLL	$1.000^{+0.160}_{-0.060}$	$1.334^{+0.201}_{-0.074}$
NNLL	$1.087^{+0.010}_{-0.001}$	$1.131^{+0.001}_{-0.014}$
N³LL	$1.119^{+0.006}_{-0.001}$	$1.130^{+0.001}_{-0.001}$

Table 1: The hard function $H(M_Z, \mu)$ at $\mu = M_Z$ for space-like and time-like choices of μ_h^2. The uncertainties are obtained by varying μ_h by a factor two about the default value.

5. Long-Distance Hadronic Effects

We model the non-perturbative effects with a Gaussian (blue) and a Dipole (red) factor in the gPDFs. The plots in Figure 4 show the impact of these effects on the intercept (top) and the peak region (bottom). By adjusting Λ_{NP} we can fit the peak region onto experimental data without influencing the measurable rest of the cross section (the intercept can not be measured at hadron colliders). Since these effects should be universal, we can set Λ_{NP} in one measurement and use it as input for other distributions. All following plots are made
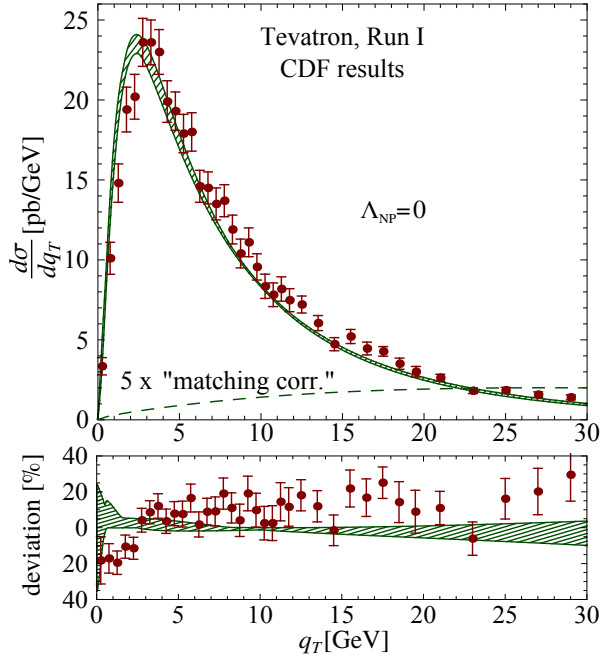
Figure 6: Comparison with data on Z-boson transverse-momentum distribution at CDF [5] without hadronic effects.
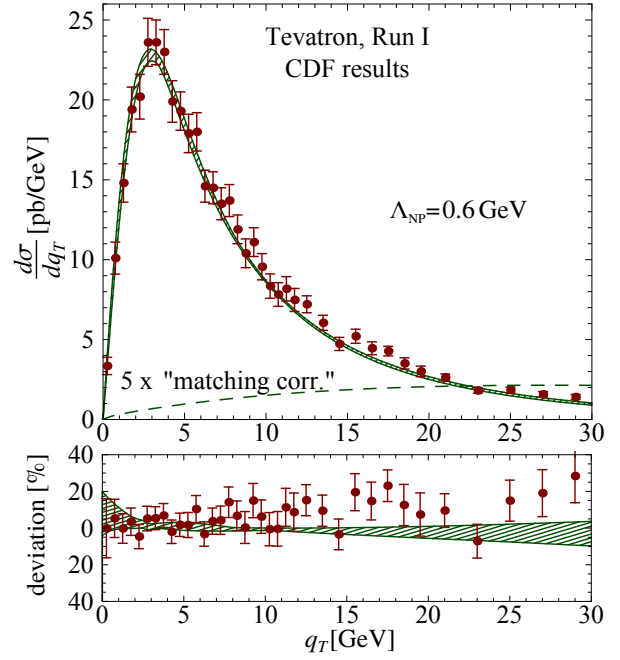

Figure 7: Comparison with data on Z-boson transverse-momentum distribution at CDF [5] with hadronic effects.

using the Gaussian model, because the differences between the two models are marginal.

Figure 5 shows the same plots in the Higgs case. The effects are strongly suppressed compared to the Z-boson production in Figure 4. The DY-like cross sections are protected from receiving large long-distance hadronic contributions by the CA. The effects scale with the ratio Λ_{NP}/q_*, which is much smaller in Higgs production.

6. Final Results

The last two plots show our final results, comparisons with data on Z-boson transverse-momentum distribution at CDF [5], Figure 6 without and Figure 7 with hadronic effects. Including these effects obviously improves the agreement of theory and data at small q_T, while it does not influence the predictions above $q_T \approx 15\,\text{GeV}$. By using SCET we miss terms of $O(\lambda^2)$, which become important at large q_T. To receive a result for the whole q_T-region, we match our result onto fixed-order calculations. The deviation at larger q_T arises because we only include matching at NLO fixed-order and should be reduced at NNLO. The matching correction is shown five times larger to make it visible.

7. Conclusion

As shown in the last plots, our approach of factorizing the DY-like cross sections, using SCET and resumming large logarithms via RG-methods, leads to very good agreement of theory predictions and experimental data, together with small scale uncertainties. There have been a lot of approaches since the first resummation [6] in 1985, but this is the first time it was done directly in momentum space and it is free of Landau-pole singularities. Two important advantages of this approach are, it is straightforward to extend the calculation to higher orders in α_s and λ and the used methods are process independent, therefore applicable to other problems [7].

References

[1] S. Drell and T.-M. Yan. Phys.Rev.Lett. **25** (1970) 316–320.
[2] T. Becher, M. Neubert, and D. Wilhelm. JHEP **1202** (2012) 124, `arXiv:1109.6027 [hep-ph]`.
[3] C. W. Bauer, S. Fleming, D. Pirjol, and I. W. Stewart. Phys.Rev. **D63** (2001) 114020, `arXiv:hep-ph/0011336 [hep-ph]`.
[4] V. Sudakov. Sov.Phys.JETP **3** (1956) 65–71.
[5] T. Affolder *et al.* Phys.Rev.Lett. **84** (2000) 845–850, `arXiv:hep-ex/0001021 [hep-ex]`.
[6] J. C. Collins, D. E. Soper, and G. F. Sterman. Nucl.Phys. **B250** (1985) 199.
[7] T. Becher and M. Neubert. JHEP **1207** (2012) 108, `arXiv:1205.3806 [hep-ph]`.